Probabilistic Estimation of Critical Flaw Sizes in the Primary Structure Welds of the Ares I–X Launch Vehicle

S.S. Pai
Glenn Research Center, Cleveland, Ohio

P.A. Hoge, B.M. Patel, and V.K. Nagpal
N&R Engineering, Cleveland, Ohio

NASA STI Program . . . in Profile

Since its founding, NASA has been dedicated to the advancement of aeronautics and space science. The NASA Scientific and Technical Information (STI) program plays a key part in helping NASA maintain this important role.

The NASA STI Program operates under the auspices of the Agency Chief Information Officer. It collects, organizes, provides for archiving, and disseminates NASA's STI. The NASA STI program provides access to the NASA Aeronautics and Space Database and its public interface, the NASA Technical Reports Server, thus providing one of the largest collections of aeronautical and space science STI in the world. Results are published in both non-NASA channels and by NASA in the NASA STI Report Series, which includes the following report types:

- TECHNICAL PUBLICATION. Reports of completed research or a major significant phase of research that present the results of NASA programs and include extensive data or theoretical analysis. Includes compilations of significant scientific and technical data and information deemed to be of continuing reference value. NASA counterpart of peer-reviewed formal professional papers but has less stringent limitations on manuscript length and extent of graphic presentations.

- TECHNICAL MEMORANDUM. Scientific and technical findings that are preliminary or of specialized interest, e.g., quick release reports, working papers, and bibliographies that contain minimal annotation. Does not contain extensive analysis.

- CONTRACTOR REPORT. Scientific and technical findings by NASA-sponsored contractors and grantees.

- CONFERENCE PUBLICATION. Collected papers from scientific and technical conferences, symposia, seminars, or other meetings sponsored or cosponsored by NASA.

- SPECIAL PUBLICATION. Scientific, technical, or historical information from NASA programs, projects, and missions, often concerned with subjects having substantial public interest.

- TECHNICAL TRANSLATION. English-language translations of foreign scientific and technical material pertinent to NASA's mission.

Specialized services also include creating custom thesauri, building customized databases, organizing and publishing research results.

For more information about the NASA STI program, see the following:

- Access the NASA STI program home page at *http://www.sti.nasa.gov*

- E-mail your question via the Internet to *help@sti.nasa.gov*

- Fax your question to the NASA STI Help Desk at 443–757–5803

- Telephone the NASA STI Help Desk at 443–757–5802

- Write to:
  NASA Center for AeroSpace Information (CASI)
  7115 Standard Drive
  Hanover, MD 21076–1320

GT2008–50626

Probabilistic Estimation of Critical Flaw Sizes in the Primary Structure Welds of the Ares I–X Launch Vehicle

S.S. Pai
Glenn Research Center, Cleveland, Ohio

P.A. Hoge, B.M. Patel, and V.K. Nagpal
N&R Engineering, Cleveland, Ohio

National Aeronautics and
Space Administration

Glenn Research Center
Cleveland, Ohio 44135

Level of Review: This material has been technically reviewed by technical management.

Probabilistic Estimation of Critical Flaw Sizes in the Primary Structure Welds of the Ares I–X Launch Vehicle

S.S. Pai
National Aeronautics and Space Administration
Glenn Research Center
Cleveland, Ohio 44135

P.A. Hoge, B.M. Patel, and V.K. Nagpal
N&R Engineering
Cleveland, Ohio 44130

Summary

The primary structure of the Ares I–X Upper Stage Simulator (USS) launch vehicle is constructed of welded mild steel plates. There is some concern over the possibility of structural failure due to welding flaws. It was considered critical to quantify the impact of uncertainties in residual stress, material porosity, applied loads, and material and crack growth properties on the reliability of the welds during its pre-flight and flight. A criterion—an existing maximum size crack at the weld toe must be smaller than the maximum allowable flaw size—was established to estimate the reliability of the welds. A spectrum of maximum allowable flaw sizes was developed for different possible combinations of all of the above listed variables by performing probabilistic crack growth analyses using the ANSYS finite element analysis code in conjunction with the NASGRO crack growth code.

Two alternative methods were used to account for residual stresses: (1) The mean residual stress was assumed to be 41 ksi and a limit was set on the net section flow stress[1] during crack propagation. The critical flaw size was determined by parametrically increasing the initial flaw size and detecting if this limit was exceeded during four complete flight cycles, and (2) The mean residual stress was assumed to be 49.6 ksi (the parent material's yield strength) and the net section flow stress limit was ignored. The critical flaw size was determined by parametrically increasing the initial flaw size and detecting if catastrophic crack growth occurred during four complete flight cycles.

Both surface-crack models and through-crack models were utilized to characterize cracks in the weld toe.

1.0 Introduction and Objectives

The primary structure of the Upper Stage Simulator of the Ares I–X launch vehicle consists of several welded steel components called CANS that will be subjected to a variety of loading conditions during its intended service life. Preliminary deterministic analyses do not account for the significant uncertainties involved (particularly the residual stresses induced from the welding process). The probabilistic analysis reported herein was undertaken in order to capture the impact of key uncertainties. The most important criterion is the size of the initial weld flaw that renders the structure seriously vulnerable to failure during its solo flight. If this critical flaw size is smaller than the resolution of the flaw detection equipment, then a serious reliability issue arises.

Deterministic analyses generally assume a value for a "factor-of-safety" to roughly account for uncertainties. This approach, however, fails to yield quantitative reliability values and often leads to designs that are either overly conservative or too risky. This is especially true for unconventional or new designs that lack a relevant reliability database. This is the situation we have with the USS primary structure where the structural integrity of the welds is not within the known empirical database and theoretical reliability models are not straightforward using traditional deterministic methods. Hence, it is prudent to utilize a probabilistic analysis to capture the impact of the uncertainties on reliability. As an added benefit, probabilistic analyses also identify the most important uncertainties, which provide project managers the key information needed to allocate resources wisely to improve reliability.

The specific technical goals of the probabilistic analyses were:

(1) Quantify the effect of the design variables, loads, and material properties and their uncertainties on crack growth.

(2) Evaluate the sensitivity of the stress field due to uncertainties.

(3) Determine the worst case probabilistic stress field range due to the range of uncertainties and their effect on crack growth.

(4) Quantify the effects of cracks and residual stresses at the toe of the shell-to-flange weld on the primary structure life.

1.1 Description of the USS Primary Structure

The Ares I–X USS is comprised of several cylindrical "tuna cans," hereinafter referred to as CANS, which are fabricated from steel plate (ASTM A516 Grade 70) as shown in Figure 1. The CANS are labeled IS–1, IS–2, SR, US–1, US–2, US–3, US–4, US–5, US–6, US–7, SA and SM. Each of the CANS is

---

[1]"Flow stress limit" represents the average of the material's yield strength and ultimate strength.
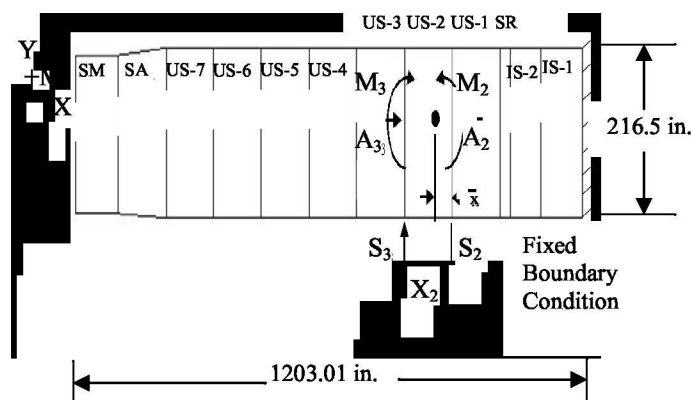
Figure 1.—Ares I-X USS primary structural components.

formed in a cylindrical shape with circular disk-shaped flanges welded to it at both ends. CANS US–2 through US–7 are the same size in height (115.5 in.), diameter (215.5 in. inner diameter), and casing thickness (0.5 in.). CANS IS–1, IS–2, SR, and US–1 differ in their height dimensions (100, 72, 24.08, and 117 in., respectively) but contain the same constant diameter, except for CANS SA and SM located at the top of the stack-up. SM is smaller in diameter (197 in. inner diameter) and SA tapers in diameter to transition from US–7 to SM. Each of the CANS cylindrical walls are 0.5 in. thick, while all the mating flanges are 1 in. thick and 6 in. wide.

The CANS are attached to each other with 7/8 in. diameter bolts through the flanges at 2° increments. The centers of the bolts are located along a 212.5 in. diameter circle. Thus, a total of 180 bolts connect adjoining pairs of CANS. Gusset plates (12 high by 5.5 wide by ½ in. thick) are located at 10° increments between the bolt locations.

2.0 Loads

The Ares I–X USS is subjected to the following five load conditions, handling loads, rollout loads, pre-launch loads, launch loads, and max-Q loads.

The load application methodology is discussed with US–2 as an example. Figure 1 details the load application for the US–2 component where A_3, S_3, and M_3 are the applied axial, applied shear, and applied moment at the left of US–2, respectively. A_2, S_2 and M_2 are the resultant axial, resultant shear, and resultant moment at the right of US–2 and at the left of US–1.

3.0 Finite Element Modeling

A coarse-mesh global finite element model of the entire USS primary structure was obtained from NASA along with the applied loads. Each CAN's shell is modeled with plate elements 3.76 in. wide by 6.06 in. long. Such a coarse model does not allow the capture of peak stress values within a narrow region. Hence, a 12° sector fine-mesh sub-model was created to substantially increase fidelity in the region of the
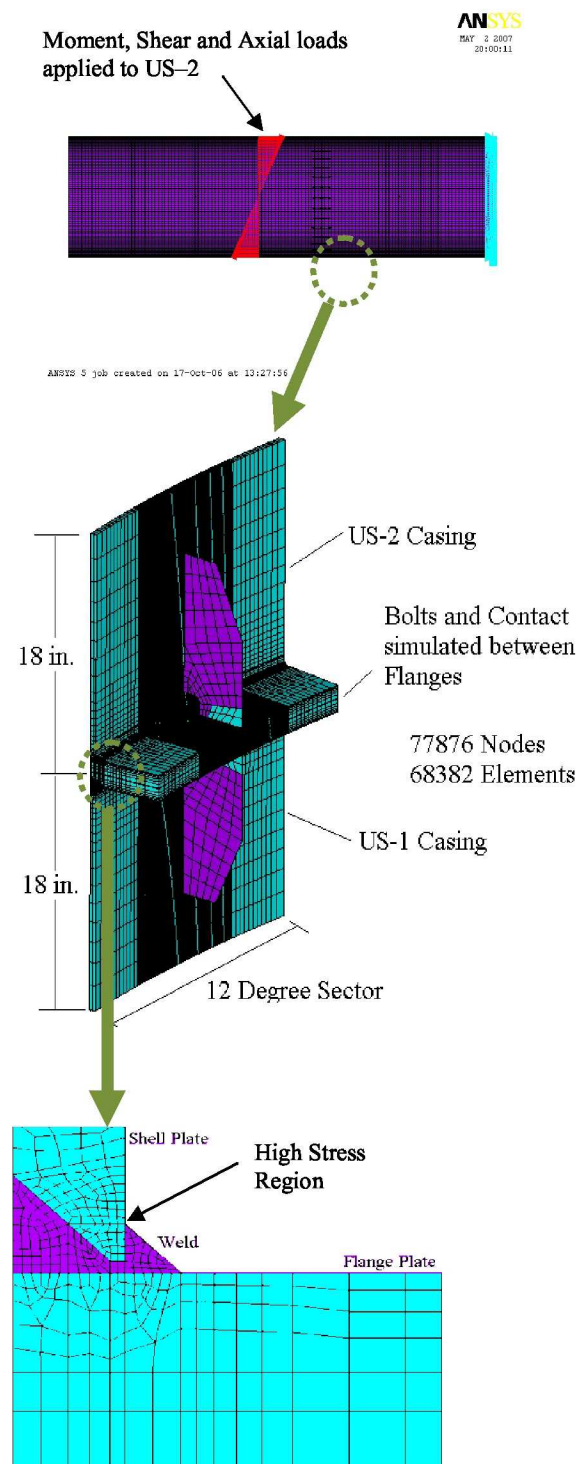

Figure 2.—Global model to sub-model with cross section mesh detail at flange to cylinder shell interface

peak stress identified by the global model analysis; namely, the fillet weld toe adjacent to the shell casing of CAN US–2 (Fig. 2). This modeling transition was accomplished using the physics-based ANSYS global-to-sub-model technique (Ref. 1).

From the analyses of the global models, the maximum stress was found to exist in CAN US–2 during the launch load condition. The location was identified as shown in Figure 2 near the toe of the fillet weld at the shell casing. A surface flaw at the weld toe is assumed to grow in the radial direction through the shell casing and in the circumferential direction along the inner diameter of the casing. The flaw will propagate normal to the primary stress field which was found to be in the axial direction along the shell casing perpendicular to the flange plate.

The sub-model for the selected region was created using a 12° symmetric section centered about a gusset plate in the circumferential direction (see Fig. 2). This high-stress local region of the structure was modeled with a fine mesh, which gradually transitions to an even finer mesh encompassing the area of interest—the location of the maximum stress value.

The sub-model contains the flanges, CAN shell casings, and weld between the shell and flanges modeled using 8-node brick elements. The meshing of the welds and the base metal near the weld area of interest is kept very fine (approx. 1/32 in. in length and width (see Fig. 2)). The gusset plates were modeled with shell elements.

The bolts that connect the flanges of CANS US–1 and US–2 of the sub-model are modeled using beam elements. A pre-strain value of 0.0022 in.[2] was applied to each of the bolt elements to simulate the tightening effect of the bolts by torque. Contact between the mating surfaces of the sub-model flanges of the adjacent CANS was simulated as well.

Applying the sub-model technique, the global model was first analyzed to simulate the loading condition and deformation shape. The displacement values from the deformed shape of the global model were applied to the sub-model edges (i.e., along the cut boundary). This displacement boundary condition assures that there exists compatibility of the displacements at the boundary of the sub-model with its matching geometry of the global model; that is, no gap or overlap exists at the boundary cut from the deformed shape of the global model. This assures that the stress field will also be compatible with the global model except that it represents a refinement of the analysis to capture the peak stresses in the region of the sub-model without neglecting the overall behavior of the global structure.

4.0 Stress Analyses Procedure Using ANSYS

Using the global finite element models of the CANS and the sets of provided loads, preliminary analyses were performed for each CAN for each load condition. From these results, it was concluded that CAN US–2 exhibited the highest stress value at the weld near the junction of the flange and its shell (see Figs. 2 and 3) for the launch load condition.

Initial probabilistic analyses revealed that stresses were much more sensitive to the applied load uncertainties than uncertainties in Young's Modulus and Poisson's ratio. Hence subsequent analyses focused on the uncertainties in the applied loads, residual stress, fracture toughness, and crack growth rate constant of the NASGRO Equation (2). Later sensitivity results show that residual stress is the dominant variable when the flow stress is not exceeded during crack propagation. However, when the flow stress limit is exceeded, the fracture toughness becomes dominant.

Representative results show that the mean values of the critical flaw size were 2.56 in. long along the surface and 0.416 in. deep through the 0.5 in. shell thickness with 41 ksi residual stress for Method 1 (flow stress limit not exceeded), and 3.12 in. long and 0.44 in. deep with 49.6 ksi residual stress for Method 2 (flow stress limit exceeded) as defined previously. These values are well beyond the minimum flaw detection criteria in welding inspection; hence, these representative flaw sizes should be easily detectable by NDE equipment or even by visual inspection. Note that these specific crack dimensions should not be used as the permissible crack sizes for welding inspection.

After the global analyses were completed the sub-model technique was applied for each load case to capture the peak longitudinal stresses. The displacement boundary conditions captured from the global analyses were applied to the cut boundary of the sub-model as described previously.

The USS was analyzed for all five load conditions to generate the maximum and minimum stresses due to the applied reversible loads at the critical stress location shown in Figure 3 (toe of the fillet weld at the shell casing). This represents the location for the maximum stress due to the governing launch load. The stress values for all five load conditions were recorded using the mean values of Young's Modulus, Poisson's Ratio, porosity, and loads. Next, the stress values due to the perturbed range of these variables were recorded for each case defined by the maximum and minimum values of the fore mentioned variables each used in separate cases. Residual stresses were not included in the tabulated stress values recorded from the ANSYS results, but are added to the listed stress values for the mean case using NASGRO.

Figure 3.—Maximum principal stress (psi) for launch load in CAN US–2.
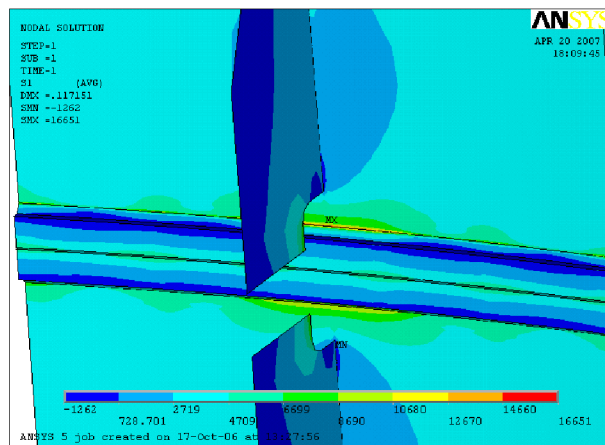
5.0 Crack Growth Analyses Assumptions

The results of the probabilistic stress analyses indicate that the stress response values are not nearly as sensitive to Young's Modulus, Poisson's Ratio, or porosity as compared to the loads. Therefore to simplify the complexity of the crack growth analyses it was decided to ignore these variables in the sensitivity portion of the crack analyses. For the NASGRO analyses the loads, residual stresses, fracture toughness, and the NASGRO crack growth rate constant were considered as independent variables in the probabilistic crack analyses and corresponding sensitivity analyses. Property values for the NASGRO analysis were obtained under the direction of NASA as well as References 3 and 4.

Crack growth analyses were performed using the NASGRO program. An initial flaw was assumed to propagate through the shell plate in the direction normal to the applied stress at the weld toe (refer to Fig. 2 and Refs. 5 and 6). The thickness of each CAN's shell casing is 0.5 in. through which a flaw may propagate.

Two NASGRO crack growth models (SC17 and TC01) were considered for the crack growth analyses. The NASGRO program allows for crack growth calculations when the net section flow stress is exceeded, as is the case when the residual stress reaches the material yield strength.

The loading cycles for the crack growth analyses were applied using NASGRO. A sample schematic of the load cycles for all loading conditions is given in Figure 4. A single load flight schedule is defined as the total accumulation of load cycles the vehicle will be subjected to during all 5 phases: handling, rollout, the pre-launch condition, launch, and flight. All the load cycles are consolidated in NASGRO within a single flight schedule. Note that not all of the rollout and pre-launch load cycles are shown in the Figure 4 schematic.

The maximum residual stresses were assumed at 49.6 ksi with an uncertainty of ±10 percent. These stresses were distributed only within a 1/8 in. section of the thickness, and then sharply transitioned to zero at 1/4 in. depth (midpoint of the shell thickness). The maximum value of 49.6 ksi reduces linearly to zero within this distance. A schematic of the typical residual stress profile used is provided in Section 6. It was considered to use a residual stress profile that contained compressive stresses in addition to the tensile field to satisfy equilibrium, however, it was deemed conservative and fitting for this analysis to use a value of zero for the region where compressive stresses may exist (Ref. 7). Assuming the maximum value of residual stress, the total stress value exceeds the flow stress criterion which is half of the sum of yield strength plus ultimate strength.

The typical stress distribution retrieved from the ANSYS FEA results is shown in Figure 5.

Another study of the stress distribution assumed a similar residual stress profile of 41 ksi with ±10 percent uncertainties using an initial crack depth of 0.1 in. This stress profile avoids exceeding the flow stress limit criterion.
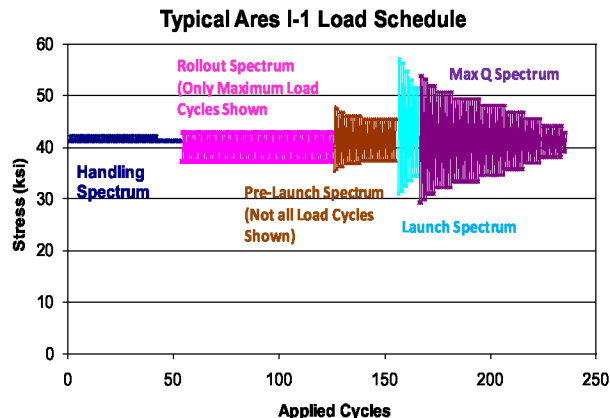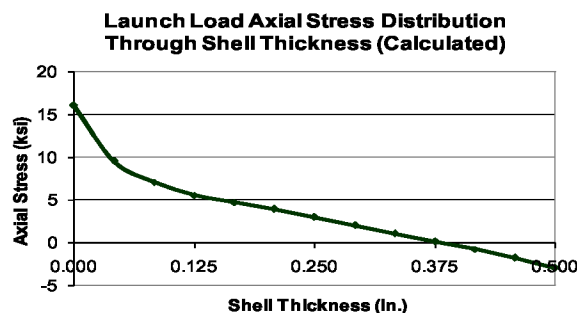

Figure 4.—Load cycles for all types of loading.

Figure 5.—Applied stress distribution profile due to launch load through shell thickness.

6.0 Results of the NASGRO Probabilistic Analyses

NASGRO analyses were performed to study the surface crack and through crack growths using the SC17 and TC01 models (Ref. 2). These analyses compared favorably to those performed by NASA and NESC. Critical Initial Flaw Sizes (crack sizes at four flight schedules before the crack becomes unstable) were determined for three sets of assumptions (Ref. 8):

6.1—Surface Crack analyses for comparison to NASA and NESC results and for probabilistic analyses—flow stress *not* exceeded.

6.2—Surface Crack analysis for comparison to NASA and NESC results and for probabilistic analyses allowing flow stress to be exceeded.

6.3—Through Crack analysis for comparison to NASA and NESC results and for probabilistic analyses allowing flow stress to be exceeded.

A summary of the random variables and their statistics used for the probabilistic analysis is provided in Table 1. The probabilistic analysis was performed using the NESSUS software.

TABLE 1.—INDEPENDENT VARIABLES FOR PROBABILISTIC
CRACK GROWTH ANALYSIS

Variables	Label	Mean[a]	Positive	Negative	Uncertainties, percent
Load as a set: L (six load cases[b])	L	1.43	1.5015	1.4014	±5
Residual stress: RS 1 (ksi)	RS	49.6	54.56	44.64	±10
Residual stress: RS 2 (ksi)	RS	41	45.1	36.9	±10
Crack growth constant: C	C	7.0E-10	7.7E-10	6.3E-10	±10
Fracture toughness 1: (ksi√in.)	K1c	106	116.6	95.4	±10
Material: ASTM A516 Grade 70 steel: ultimate tensile strength (Su) = 74.6 ksi; yield strength (Sy) = 49.6 ksi					

[a]Normal distribution assumed for all variables
[b]Represented as the weighted average of stress range: $\Sigma S_i N_i / \Sigma S_i \Longrightarrow$
S_i = Stress range; N_i = no. of cycles

TABLE 2.—PROBABILISTIC CRACK SIZE RESULTS
FOR CASE 6.1

Group	Variable	Uncertainty, percent	Flight schedules	Final crack depth "a", in.	Final crack length "2c", in.
1	Mean	0	300	0.4176	2.606
2	L	5	259	.4095	2.524
3	L	−5	361	.4284	2.689
4	RS	10	265	.3783	2.082
5	RS	−10	698	.5000	6.326
6	C	10	272	.4164	2.589
7	C	−10	334	.4185	2.618
8	K1c	10	306	.4188	2.614
9	K1c	−10	293	.4169	2.607

Mean   mean values of all variables
L   loads
RS   residual stress
C   crack growth rate constant
K1c   fracture toughness
All NASGRO results are tabulated with four flight schedules remaining

6.1 Surface Crack With Flow Stress Not Exceeded

The results of surface crack analyses using NASGRO model SC17 and without violating the flow stress limit are displayed in Table 2.

The input data for the NASGRO analyses is as follows:

- NASGRO model: SC17
- a = 0.1 in. (initial flaw size)
- a/c = 0.3
- Width of the plate, w = 9 in.
- Residual stress = 41 ksi—stress profile plotted in Figure 6
- The stress is not allowed to exceed the flow stress (net section stress criteria—built within NASGRO)
- All the stresses are input from ANSYS output.

NASGRO analyses output, number of flight schedules and crack size "a" and "2c" are shown in Table 2. Note that all crack sizes "2c" range from 2.082 to 2.689, in. except for group which reaches 6.3 in. as it transitioned to a through crack model. Similarly the crack depth "a" varies from 0.378 to 0.428 in. except for Group 5 where it reaches 0.5 in., which represents the thickness of the shell. These unusual sizes are reached when the solution transitions to model TC11 which is a through crack analysis. Since TC11 ignores bending stresses, it allows the crack to be longer before it becomes unstable.

Probability analyses were performed for the response values of crack sizes "a" and "2c" and using the assumed uncertainties in the independent variables, namely K_{1c}, loads, C and residual stress. The nine groups of variables with their uncertainty values and their individual crack result

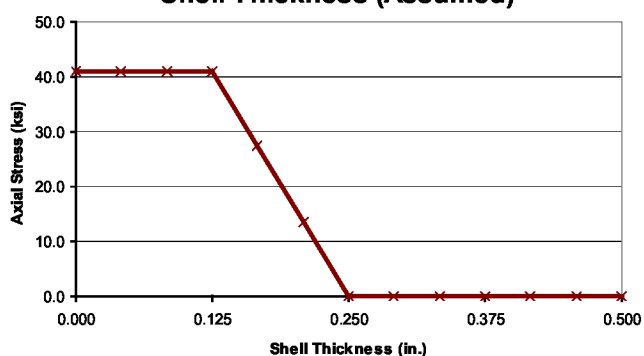**Residual Stress Distribution through Shell Thickness (Assumed)**

Figure 6.—Residual stress profile used for Case 6.1.

responses from NASGRO shown in Table 2 are input into the NESSUS code using a single input file. The cumulative distribution function and sensitivity charts are displayed in Figures 7 and 8. The output cumulative distribution functions are plotted for 13 calculated probabilities ranging from 0.0001 to 0.9999. The sensitivities are calculated at a cumulative distribution function output of 0.0001.

Results from this NESSUS run give a mean value of the crack length of 2.56 in. with a standard deviation of 0.53 in. There is a 0.001 probability chance that the crack length will remain less than 1.0 in. and a 0.999 probability chance that the crack will remain less than 4.35 in.

The cracks are very sensitive to residual stress and least sensitive to fracture toughness, K_{1c}, and slightly sensitive to loads and the crack growth rate constant.
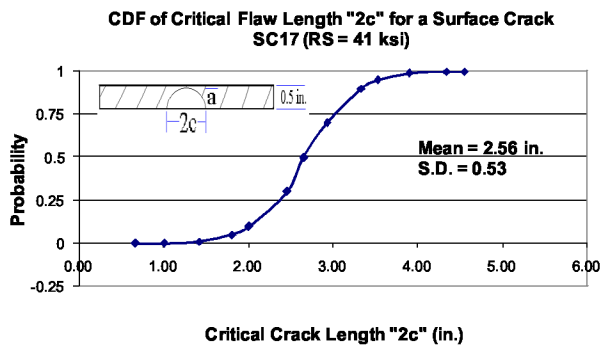
Figure 7.—Probabilistic crack size "2c" results for case 6.1 (flow stress not exceeded).
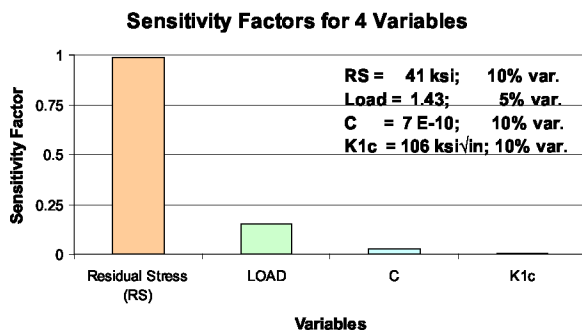

Figure 8.—Variable sensitivities for crack size "2c"—flow stress not exceeded (CDF probability level 0.0001).
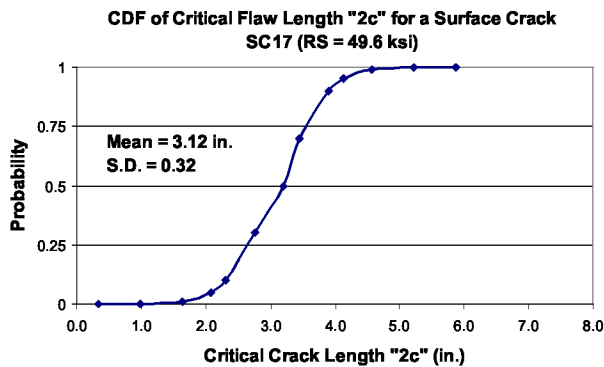

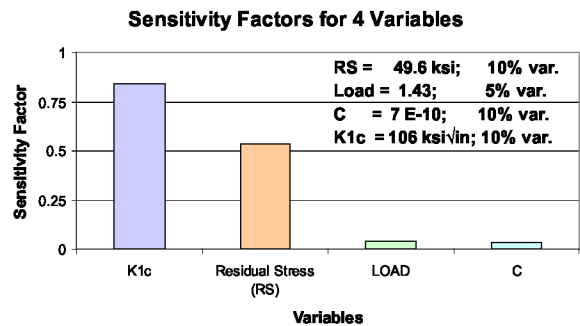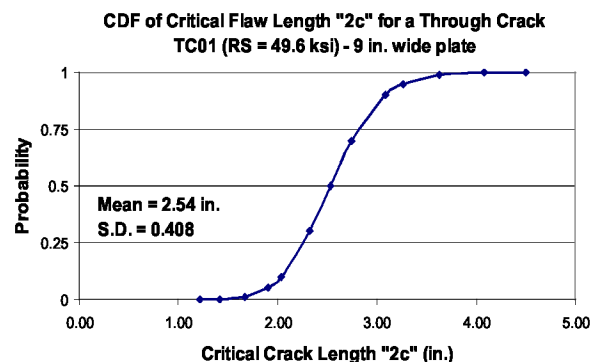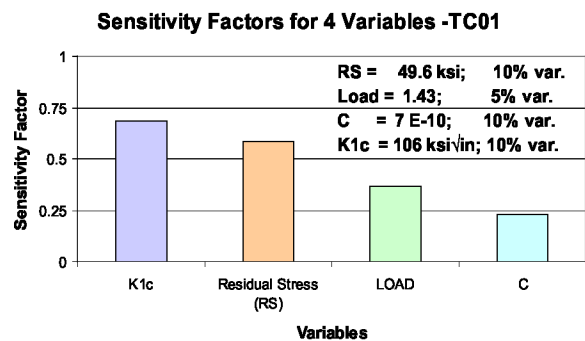Figure 9.—Probabilistic crack size "2c" results for case 6b (flow stress exceeded).

Figure 10.—Variable sensitivities for crack size "2c"—flow stress exceeded (CDF probability level 0.0001).

Figure 11.—Probabilistic crack size "2c" results for case 6c (flow stress exceeded).

Figure 12.—Variable sensitivities for crack size "2c"—flow stress exceeded (CDF probability level 0.0001).

6.2 Surface Crack Probabilistic Analyses With Stress Exceeding Flow Stress

Using similar crack growth properties and a residual stress profile as in set '6.1', a probabilistic analysis was performed using the assumptions of set '6.2' which yielded the following summarized results. The cumulative distribution function and sensitivity charts are shown in Figures 9 and 10. The mean value of the final crack length is 3.12 in. with a standard deviation of 0.32 in. There is a 0.001 probability chance that the crack length will remain less than 0.98 in. and a 0.999 probability chance that the crack length will remain less than 5.22 in.

When the analysis is allowed to exceed the flow stress within NASGRO, the crack size becomes very sensitive to fracture toughness, K_{1c} but remains fairly sensitive to the residual stress.

6.3 Through-Crack Probabilistic Analyses With Flow Stress Exceeded

A through-crack probabilistic analysis was performed using similar crack growth properties and residual stress profile as set in '6.1'. The cumulative distribution function and sensitivity charts are shown in Figures 11 and 12. When the analysis is allowed to exceed the flow stress the crack size becomes very sensitive to fracture toughness, K_{Ic} but remains

fairly sensitive to the residual stress and loads. The mean value of the crack size is 2.54 in. with a standard deviation of 0.408 in. There is a 0.001 probability chance that the crack length will remain less than 1.42 in. and a 0.999 probability chance that the crack length will remain less than 4.08 in.

7.0 Conclusions

Collectively, the foregoing results indicate that the USS primary structure should be quite reliable for its one and only flight. The calculated deterministic critical initial flaw sizes exceed 2 in. which is much greater than the resolution offered by modern flaw detection equipment. Likewise, the critical initial flaw size plots obtained from the probabilistic analysis exceed 0.98 in. for a 0.001 probability of failure.

The residual stress is the dominant variable when the flow stress is not exceeded during crack propagation. However, when the flow stress limit is exceeded, the fracture toughness becomes dominant.

Stresses are much more sensitive to the loads uncertainties than uncertainties in Young's Modulus and Poisson's ratio.

References

1. Whitcomb, J.D., Woo, K., "Application of Iterative Global/Local Finite-Element Analysis. Part I: Linear Analysis," Aerospace Engineering Department, Texas A&M University, College Station, Texas, 1993.

2. Southwest Research Institute, *NASGRO Reference Manual*, Version 5.0, July 2006.

3. McKeighan, P.C. and Hudak, Jr. S.J., "Summary of Material Property References for Structural Steels and Recommended for Use in Tank Car Stub-Sill Damage Tolerance Analysis," Materials Engineering Department, Southwest Research Institute, June 1996.

4. Womack, J., "Bounds for Fracture Toughness," *Tolerance Bounds for Fracture Toughness,* NASA Glenn Research Center, Cleveland, July 2007.

5. Hudak, Jr. S.J., Burnside, O.H., and Chan, K.S., "Analysis of Corrosion Fatigue Crack Growth in Welded Tubular Joints," *Journal of Energy Resources Technology*, June, 1985, Southwest Research Institute, San Antonio, Texas.

6. Cardinal, J.W., McKeighan, P.C., and Hudak, Jr. S.J., "Damage Tolerance Analysis of Tank Car Stub Sill Cracking," SwRI Final Report Project No. 06-6965, Southwest Research Institute, San Antonio, Texas, November, 1998.

7. NESC, "Surface Crack Stress Intensity Factor Comparison," NASA Langley Research Center, Hampton, Virginia, August 2007.

8. McClung, C., Riha, D., "Draft Guidelines for Probabilistic Fracture Mechanics Analysis," Southwest Research Institute, San Antonio, June 2007.

REPORT DOCUMENTATION PAGE

Form Approved
OMB No. 0704-0188

1. REPORT DATE *(DD-MM-YYYY)* 01-11-2009	2. REPORT TYPE Technical Memorandum	3. DATES COVERED *(From - To)*

4. TITLE AND SUBTITLE
Probabilistic Estimation of Critical Flaw Sizes in the Primary Structure Welds of the Ares I-X Launch Vehicle

5a. CONTRACT NUMBER

5b. GRANT NUMBER

5c. PROGRAM ELEMENT NUMBER

6. AUTHOR(S)
Pai, S., S.; Hoge, P., A.; Patel, B., M.; Nagpal, V., K.

5d. PROJECT NUMBER

5e. TASK NUMBER

5f. WORK UNIT NUMBER
WBS 136905.10.10.80.20.40.01

7. PERFORMING ORGANIZATION NAME(S) AND ADDRESS(ES)
National Aeronautics and Space Administration
John H. Glenn Research Center at Lewis Field
Cleveland, Ohio 44135-3191

8. PERFORMING ORGANIZATION REPORT NUMBER
E-16824

9. SPONSORING/MONITORING AGENCY NAME(S) AND ADDRESS(ES)
National Aeronautics and Space Administration
Washington, DC 20546-0001

10. SPONSORING/MONITOR'S ACRONYM(S)
NASA

11. SPONSORING/MONITORING REPORT NUMBER
NASA/TM-2009-215583; GT2008-50626

12. DISTRIBUTION/AVAILABILITY STATEMENT
Unclassified-Unlimited
Subject Categories: 39, 15, 18, and 05
Available electronically at http://gltrs.grc.nasa.gov
This publication is available from the NASA Center for AeroSpace Information, 443-757-5802

13. SUPPLEMENTARY NOTES

14. ABSTRACT
The primary structure of the Ares I-X Upper Stage Simulator (USS) launch vehicle is constructed of welded mild steel plates. There is some concern over the possibility of structural failure due to welding flaws. It was considered critical to quantify the impact of uncertainties in residual stress, material porosity, applied loads, and material and crack growth properties on the reliability of the welds during its pre-flight and flight. A criterion--an existing maximum size crack at the weld toe must be smaller than the maximum allowable flaw size--was established to estimate the reliability of the welds. A spectrum of maximum allowable flaw sizes was developed for different possible combinations of all of the above listed variables by performing probabilistic crack growth analyses using the ANSYS finite element analysis code in conjunction with the NASGRO crack growth code. Two alternative methods were used to account for residual stresses: (1) The mean residual stress was assumed to be 41 ksi and a limit was set on the net section flow stress during crack propagation. The critical flaw size was determined by parametrically increasing the initial flaw size and detecting if this limit was exceeded during four complete flight cycles, and (2) The mean residual stress was assumed to be 49.6 ksi (the parent material's yield strength) and the net section flow stress limit was ignored. The critical flaw size was determined by parametrically increasing the initial flaw size and detecting if catastrophic crack growth occurred during four complete flight cycles. Both surface-crack models and through-crack models were utilized to characterize cracks in the weld toe.

15. SUBJECT TERMS
Launch vehicles; Welding; Probabilistics

16. SECURITY CLASSIFICATION OF:			17. LIMITATION OF ABSTRACT	18. NUMBER OF PAGES	19a. NAME OF RESPONSIBLE PERSON STI Help Desk (email:help@sti.nasa.gov)
a. REPORT U	b. ABSTRACT U	c. THIS PAGE U	UU	13	19b. TELEPHONE NUMBER *(include area code)* 443-757-5802

Standard Form 298 (Rev. 8-98)
Prescribed by ANSI Std. Z39-18